Electronic Supplementary Material (ESI) for Journal of Materials Chemistry C.

Electronic Supplementary Information

Origin of Enhanced Efficiency and Stability in Diblock Copolymer-Grafted Cd-Free Quantum Dot-Based Light-Emitting Diodes

Yeseul Park,[a] Benjamin Klöckner,[b] Donghyo Hahm,[c] Jaehoon Kim,[a] Taesoo Lee,[a] Jaeyoul Kim,[a] Wan Ki Bae,[c] Rudolf Zentel[b] and Jeonghun Kwak[a*]

[a.] School of Electrical and Computer Engineering, Inter-university Semiconductor Research Center, Seoul National University, Seoul 08826, Republic of Korea

[b.] Institute of Organic Chemistry, Johannes Gutenberg University Mainz, Mainz D-55128, Germany

[c.] SKKU Advanced Institute of Nanotechnology (SAINT), Sungkyunkwan University, Suwon 16419, Republic of Korea

*Corresponding author Email: jkwak@snu.ac.kr (J. Kwak)

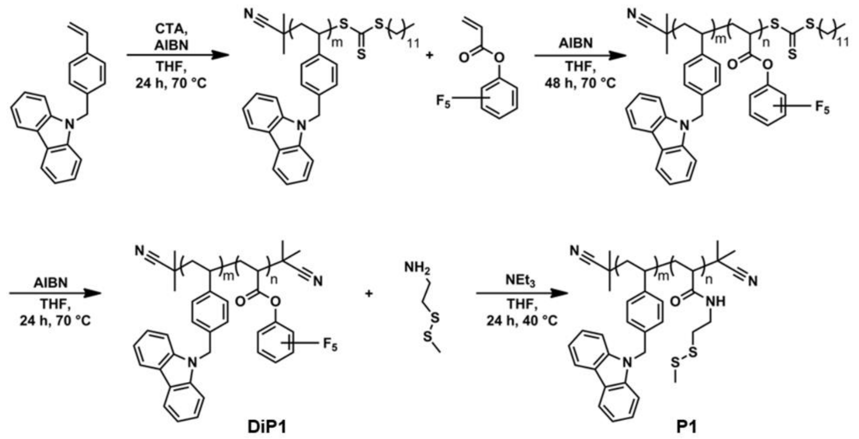

Figure S1. RAFT polymerization and post-polymerization modification for the synthesis of poly(9-(4-vinylbenzyl)-carbazole-block-cysteaminemethyldisulfide). RAFT polymerization and post-polymerization modification for the synthesis of poly(9-(4-vinylbenzyl)-carbazole-block-cysteaminemethyldisulfide. First, the homopolymer poly(9-(4-vinylbenzyl)-carbazole) was obtained by RAFT polymerization using a chain transfer agent (CTA) and used as a macro-initiator in the second RAFT polymerization of the reactive ester monomer pentafluorophenyl acetate (PFPA), leading to diblock copolymers (DiP1). The reactive ester block enables the introducing of further functionalities by a post-polymerization modification with a primary amine. After polymerization, the reactive CTA group was replaced with an inert 2-cyanoisoproyl group by reaction with excess of azobisisobutyronitrile (AIBN) to obtain defined end-groups on both sides of the polymer. During post-polymerization modification, the disulfide anchor groups were introduced into the polymer by reaction with the reactive units in the PFPA block, leading to the diblock copolymer poly(9-(4-vinylbenzyl)-carbazole-block-cysteaminemethyldisulfide (P1).

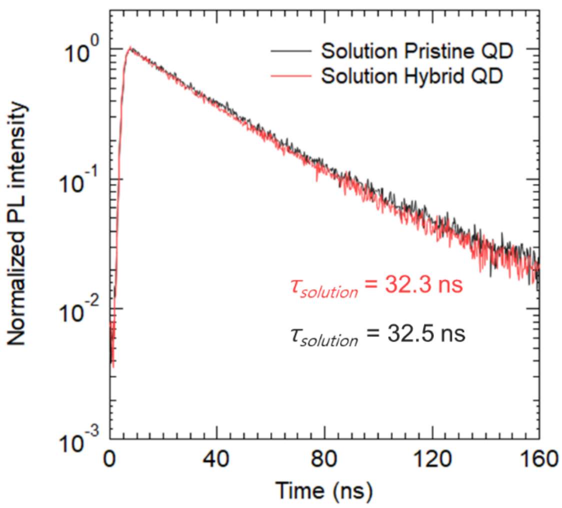

Figure S2. TRPL decay curves of the pristine and hybrid QDs in solution.

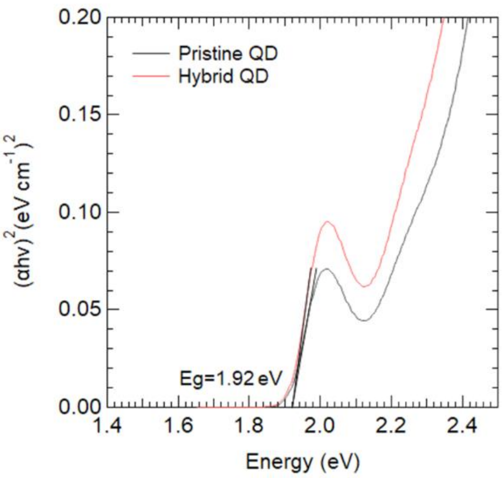

Figure S3. Touc plot of the pristine and hybrid QDs, showing that both QDs have similar optical band gap of ~1.92 eV.

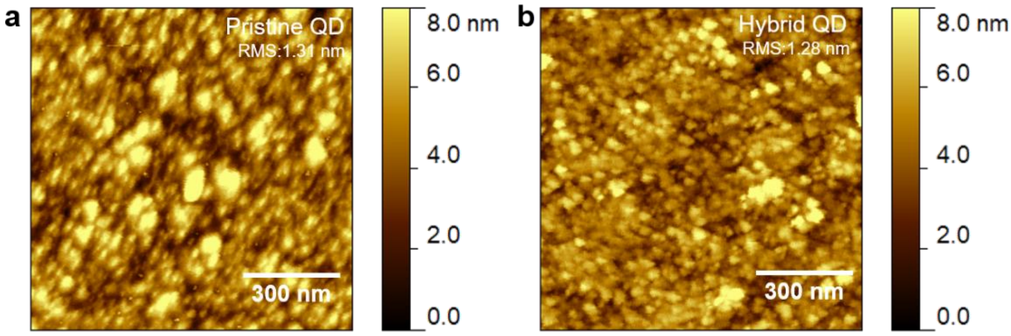

Figure S4. AFM images of (a) pristine and (b) hybrid QDs films.

a

Device	QD : Polymer
Pristine QD	1:0
Hybrid (A)	1:0.25
Hybrid (B)	1:0.375
Hybrid (C)	1:0.5
Hybrid (D)	1:0.75

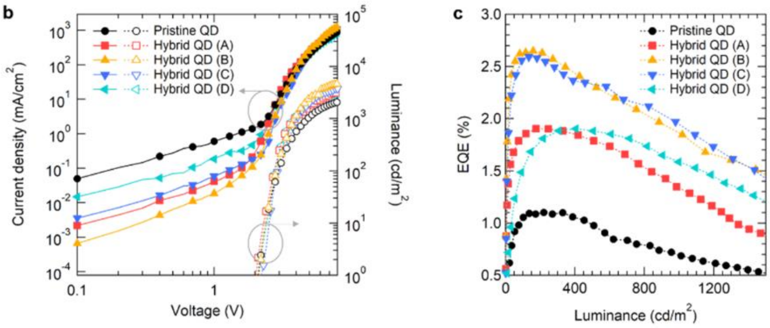

Figure S5. (a) Device configuration table, (b) *J*–*V*–*L* characteristics, and (c) EQE curves of the QLEDs with various QD–polymer ratios.

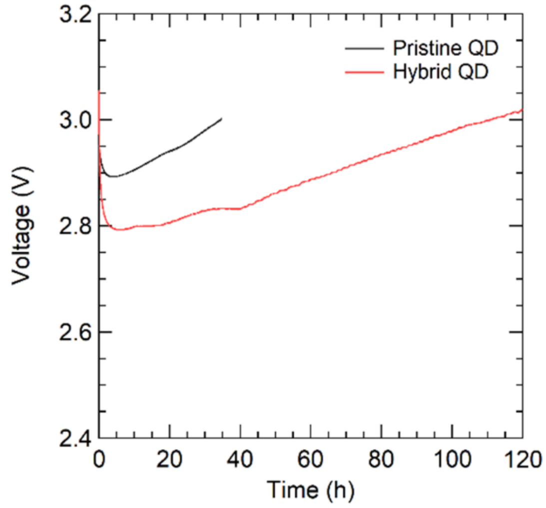

Figure S6. Driving voltage change over time at an initial luminance of 1000 cd/m^2.

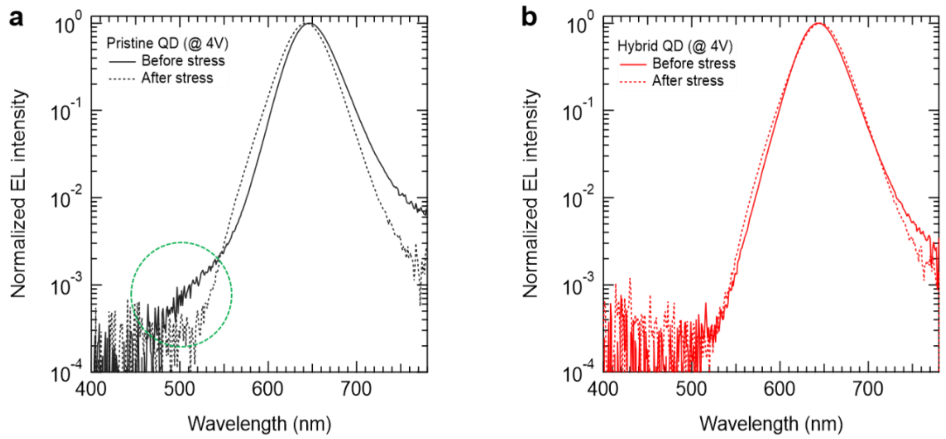

Figure S7. Normalized EL spectra (measured at 4 V) of the QLEDs using the (a) pristine QDs and (b) hybrid QDs before and after bias stress.

Table S1. Performances of the QLEDs with the pristine and hybrid QDs.

QDs	**EL peak wavelength (nm)**	**V_{on} (V) (at 1 cd/m^2)**	**Max. EQE (%)**	**Max. PE (lm/W)**	**Max. *L* (cd/m^2)**	**T_{50} (h) (@ L_0 = 1000 cd/m^2)**
Pristine QD	632	1.9	2.5	2.8	4,200	30
Hybrid QD	632	1.8	3.7	4.8	4,500	120

Table S2. Parameters for the impedance analysis of the HODs with the hybrid and pristine QDs upon degradation.

HOD		*Rs* (Ω)	*Rp* (Ω)	*Cp* (nF)
Pristine QD	Before stress	140	10570	1.06
	After stress	148 (▲5.7%)	13300 (▲25.8%)	1.08 (▲1.9%)
Hybrid QD	Before stress	110	1785	1.04
	After stress	111 (▲0.9%)	1872 (▲4.9%)	1.05 (▲1.0%)